frontiers in Materials

ORIGINAL RESEARCH
published: 26 May 2021
doi: 10.3389/fmats.2021.674287

Zeolite-Loaded Titanium Dioxide Photocatalytic Cement-Based Materials for Efficient Degradation of Drinking Water Disinfection Byproduct Trichloroacetamide

Gang Liao[1], Anming She[1,2], Wenhai Chu[3], Junqing Zuo[4] and Wu Yao[1,2]*

[1] School of Materials Science and Engineering, Tongji University, Shanghai, China, [2] Key Laboratory of Advanced Civil Engineering Materials of Ministry of Education, Tongji University, Shanghai, China, [3] State Key Laboratory of Pollution Control and Resources Reuse, College of Environmental Science and Engineering, Tongji University, Shanghai, China, [4] Shanghai Construction Group Co., Ltd., Shanghai, China

OPEN ACCESS

Edited by:
Xianming Shi, Washington State University, United States

Reviewed by:
Xinjuan Liu, China Jiliang University, China
Abdul Rahman Mohamed, Universiti Sains Malaysia (USM), Malaysia

***Correspondence:**
Anming She
sheanming@tongji.edu.cn

Specialty section:
This article was submitted to Structural Materials, a section of the journal Frontiers in Materials

Received: *01 March 2021*
Accepted: *19 April 2021*
Published: *26 May 2021*

Citation:
Liao G, She A, Chu W, Zuo J and Yao W (2021) Zeolite-Loaded Titanium Dioxide Photocatalytic Cement-Based Materials for Efficient Degradation of Drinking Water Disinfection Byproduct Trichloroacetamide. Front. Mater. 8:674287. doi: 10.3389/fmats.2021.674287

A two-step method was used to load TiO_2 on a cement matrix, and zeolite was chosen as intermediate support. TiO_2@Zeolite composite coated photocatalytic cement-based material (PCM) was prepared. Some advanced characterization technologies including X-ray diffraction (XRD), scanning electronic microscopy (SEM), energy dispersive X-ray spectroscopy (EDS), and BET specific surface area (SSA) test were applied to characterize the physicochemical properties of as-prepared PCM. Photocatalytic degradation of trichloroacetamide (TCAcAm) was conducted to evaluate its photocatalytic efficiency. Results show that TiO_2@Zeolite composite can improve the adsorption ability of PCM and TiO_2 particles were dispersed on the surface of PCM homogeneously providing abundant active sites for photocatalytic reactions. Moreover, TiO_2@Zeolite composite can reduce the negative effect of cement on TiO_2. The synergetic effect of TiO_2@Zeolite composite can remarkably improve the photocatalytic degradation rate, reaching up to 97.8%. TiO_2@Zeolite composite coated PCM holds great promise to eliminate water pollution.

Keywords: TiO_2@Zeolite composite, photocatalytic cement-based material, water purification, photocatalytic degradation, disinfection byproducts

INTRODUCTION

Nowadays, water pollution is a big environmental health concern worldwide as multiple harmful substances such as antibiotics, microbes, and dyestuffs are detected in drinking water. It is urgent to eliminate these contaminants in aqueous environments to guarantee water safety (Srogi, 2007; Ahmed et al., 2010; Zangeneh et al., 2015; Liu et al., 2017). At present, chlorine disinfection is still the main method used to disinfect tap water, since it was first applied in England in 1897, due to high disinfection efficiency, low cost, and facile implementation (Hom, 1972; Winward et al., 2008). However, some carbon-disinfection by-products (C-DBPs) will be generated in the disinfection process, which can induce many diseases like cancer (Chu et al., 2012; Chang et al., 2013). Recently, some new disinfectors such as chloramine and ozone have been developed, but

the derived nitrogen-disinfection by-products (N-DBPs) are proved to be more toxic than C-DBPs (Chu et al., 2012). Moreover, tap water is usually transported over a long distance through water supply pipes, and then stored in concrete-made water storage structures before being delivered to households, and as a result N-DBPs will concentrate and bacteria will breed fast at the end of the network (Whelton et al., 2015). Consequently, a novel strategy should be proposed to deal with these emerging challenges.

Since Fujishima and Honda found the splitting of water on a TiO_2 anode under illumination, TiO_2 has been widely studied and used in environment remediation owing to its strong photo-induced oxidation ability (Fujishima and Honda, 1972; Vinu and Madras, 2012; Wen et al., 2015; Pawar et al., 2018). In detail, active oxygen species (AOS) generated on TiO_2 like hydroxyl radical (·OH) can totally oxidize pollutants into water and carbon dioxide upon solar irradiation. Previous research has proved that heterogeneous photocatalysis exhibits specific superiority in eliminating aqueous pollutants in terms of low cost and harmless byproducts, when compared to conventional disinfection (Yoneyama and Torimoto, 2000; Karuppuchamy et al., 2007; Fuchs et al., 2009; Yamaguchi et al., 2010). Some pioneering works about using TiO_2 to purify water have been reported, which show high degradation efficiency toward pollutants. However, in most reported cases, TiO_2 has been employed in the form of nano-powder which is prone to agglomerate in aqueous environments due to its high surface energy, thus compromising its photocatalytic efficiency, and it is also difficult to recollect and reuse this powder TiO_2 (Zhang et al., 2003; Negishi et al., 2019a,b). In recent years, immobilization of TiO_2 on some support materials is promising to solve this problem, and among all support materials, cementitious material is a suitable one because of its strong binding property and chemical inertness (Chen and Poon, 2009; Jimenez-Relinque et al., 2015). So far, TiO_2-engineered photocatalytic cement-based material (PCM) has already been fabricated and applied in environment remediation such as depollution of NO_x (Seo and Yun, 2017), self-cleaning of building (Wang et al., 2014), and decomposition of volatile organic compounds (VOCs) (Aïssa et al., 2011), but few works about the application of TiO_2-incorporated PCM in water purification have been reported.

As most water storage constructions are manufactured of cement-basted materials, it is attractive to coat TiO_2 on these cement constructions to further improve drinking water quality. Although cement paste can immobilize TiO_2 particles firmly, its hydration products like C-S-H gel and Ca $(OH)_2$ can cover TiO_2, thus leading to a decline of photocatalytic activity (Chen et al., 2011). Due to the poor adsorption ability of cement matrix, only a small number of pollutant molecules will be captured by cement-based materials, which is not favorable for photocatalytic degradation reaction (Nazari and Riahi, 2011; Lee et al., 2013). So, it is of significance to reduce the negative effect of cement on photocatalysis for facilitating the application of TiO_2 coated PCM in water purification. In this paper, zeolite was selected as intermediate carrier, due to its high porosity and large specific surface area (SSA), and a two-step method was proposed to load TiO_2 on a cement matrix. Firstly, TiO_2 was dispersed and anchored on the surface of zeolite, forming TiO_2@zeolite composite. And then TiO_2@zeolite composite was coated on cement paste. Degradation of trichloroacetamide (TCAcAm) was conducted to evaluate the purification effect of the as-prepared TiO_2@zeolite composite coated PCM.

EXPERIMENTAL

Raw Materials

Conch brand P•O 42.5 cement was used in this study. Natural zeolite was produced in Henan province, China, and its chemical composition is shown in **Table 1**. All reagents including Tetrabutyl orthotitanate (TBOT), nitric acid (HNO_3), and absolute ethyl alcohol (CH_3CH_2OH) were provided by Sinopharm Chemical Reagent Co., Ltd., China.

Sample Preparation

TiO_2@Zeolite Composite Fabrication

Natural zeolite pre-treatment process: natural zeolite was washed by deionized water to eliminate impurities and heated in a 100°C drying oven for 1 h. Finally, treated zeolite was sieved by a standard sieve with a mesh number of 100. TiO_2 sol preparation process: 10 g TBOT was added into 80 g deionized water dropwise with continuous stirring, and 0.8 g HNO_3 was also incorporated to inhibit the fast hydrolysis of TBOT. After finishing adding TBOT, milky white suspension was obtained, and then thermo-treated in a 40°C water bath for 24 h, thus gaining light blue TiO_2 sol. TiO_2 loading process: 1 g zeolite was added into a certain amount of TiO_2 sol, where TiO_2 accounts for 30% weight of zeolite. Then, the mixture was stirred for 1 h and followed with a 45-min ultrasonic treatment. Finally, the mixture was placed in a vacuum reactor with a pressure of 0.07 MPa for 5 h, and then heated in a muffle furnace for 4 h at different temperatures (200, 300, 400, and 500°C), obtaining TiO_2@zeolite composite. The specimens were labeled as n-TZ, where n stands for the final thermal treatment temperature and TZ represents TiO_2@zeolite composite, for instance, 200-TZ stands for the composite treated under 200°C. For comparison, pure TiO_2 sol was dried and heated at 200°C to obtain pure TiO_2 powder.

TiO_2@Zeolite Composite Coated PCM Fabrication

22 g cement and 8.8 g water were mixed for 5 min by a mixer, and the fresh cement paste was casted in a round mold with a diameter of 50 mm and a height of 8 mm. Before the hardening of the cement paste, a certain amount of TiO_2@zeolite composite was sprayed onto the surface of the cement paste, and demolded 1 day later. All specimens were cured in a standard curing chamber (20 ± 2°C, RH ≥ 95%) for 28 d. The samples were labeled as n-TZ-m-PCM, where n stands for the final thermal treatment temperature, m% stands for the mass ratio of

TABLE 1 | Chemical composition of natural zeolite/%.

SiO_2	Al_2O_3	Na_2O	CaO	MgO	Fe_2O_3	FeO	TiO_2	K_2O	P_2O_5
60~70	17.8	4.2	2.6	0.8	1.6	1.2	0.6	3.2	0.26

TiO_2@zeolite composite to cement, TZ represents TiO_2@zeolite composite, and PCM represents PCM, for instance, 200-TZ-25-PCM represents that composite treated under 200°C was used and the composite to cement ratio was 25%. The schematic diagram of the TiO_2@zeolite composite coated PCM is shown in **Figure 1**.

Physicochemical Properties Characterization

X-ray diffraction (XRD) was used to analyze the crystal phase of as-prepared specimens, and the analysis was conducted on an X-ray diffractor equipped with a Cu Ka ray source. The diffraction angle (2θ) ranged from 10° to 80° with the interval of 0.02° at the speed of $4°min^{-1}$. Scanning electronic microscope (SEM) was applied to observe the micro-morphology of samples and energy dispersive X-ray spectroscopy (EDS) was adapted to investigate element distribution at a micro-area level. BET SSA test was used to characterize the pore structure of samples.

Photocatalytic Degradation Efficiency Characterization

TCAcAm solution preparation process: 0.5 g TCAcAm solid was added into 1 L deionized water and mixed evenly, and then the solution was diluted 100 times and the final concentration of TCAcAm solution was 5,000 μg/L. Photocatalytic degradation process: the sample was suspended in a 3 L beaker, and then 1 L of TCAcAm solution with a concentration of 5,000 μg/L was added to the beaker, and the position of the tested sample was adjusted to ensure its immersion in the TCAcAm solution. Before irradiating, the beaker containing the TCAcAm solution was placed in dark conditions for 8 h to construct the adsorption-desorption equilibrium, and then the LED lamp with a power of 12 W was switched on, and the liquid level of the solution in the beaker was 15 cm from the bottom of the light source, and 20 mL suspension was fetched at an interval of 1 h. For the control experiment, 1 L TCAcAm solution with a concentration of 5,000 μg/L was added to a 3 L beaker, but no samples were added to the beaker. The beaker was placed in the same conditions, and 20 mL suspension was fetched at the same interval. Measurement of TCAcAm concentration: the fetched suspension was filtered and transferred into a 30 mL volumetric flask by using a large-capacity pipette. And then 20 mL TCAcAm solution and 4 mL of methyl tert-butyl ether (MTBE) extractant were added to a tube, and the mixture was vibrated for 2 min by a tube shaker and placed without stirring for 5 min. Gas chromatography-mass spectrometry (GC/MS) was used to measure the TCAcAm in the upper extractant solution.

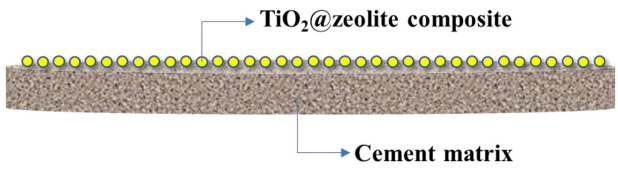

FIGURE 1 | Schematic diagram of the TiO_2@zeolite composite coated PCM.

RESULTS AND DISCUSSION

Microstructure of TiO_2@Zeolite Composite

XRD Analysis

As depicted in **Figure 2**, characteristic diffraction peaks of anatase were observed at 2θ (25.305°, 37.799°, 48.038°, 55.062°, and 62.690°) in the diffraction pattern of TiO_2 according to PDF#73-1764. This result illustrates that hydrolysis of TBOT and followed hydrothermal treatment can promote the formation of TiO_2, and TiO_2@zeolite composite based on this method will possess excellent photocatalytic activity. In the diffraction pattern of zeolite, characteristic peaks of quartz and $K_{2.04}Na_{0.06}Al_{7.8}O_{20.7}$ were observed according to PDF#89-1629, indicating zeolite was symbiotic with quartz. For the 500-TZ sample, the main crystal phases were still quartz and $K_{2.04}Na_{0.06}Al_2Si_{7.8}O_{20.7}$, suggesting that thermal treatment did not destroy the structure of zeolite. After thermal treatment, the intensity of quartz and $K_{2.04}Na_{0.06}Al_{7.8}O_{20.7}$ became stronger, indicating that its purity was improved. A weak diffraction peak was detected at 2θ (25.305°), which is the strongest diffraction peak of Anatase, confirming that TiO_2 was successfully loaded on zeolite. Due to the small amount of TiO_2 loading, only one peak of anatase was observed. And there is another possibility that because the crystalline grain size of TiO_2 was too small, the anatase diffraction intensity was weak (Jansson et al., 2015).

Micro-Morphology

As shown in **Figure 3a**, zeolite is made up of plate-like units, forming a rough surface and some micron-sized slit-like pores. This structure contributes to the capture of TiO_2 particles when immersed in TiO_2 sol, thus leading to the homogenous

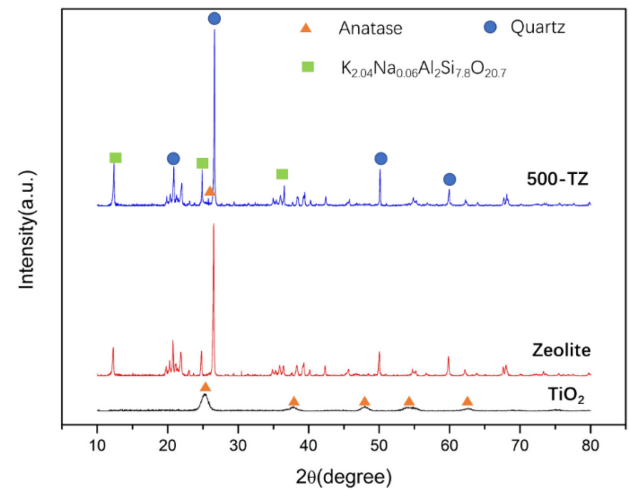

FIGURE 2 | X-ray diffraction patterns of TiO_2, Zeolite, and 500-TZ.

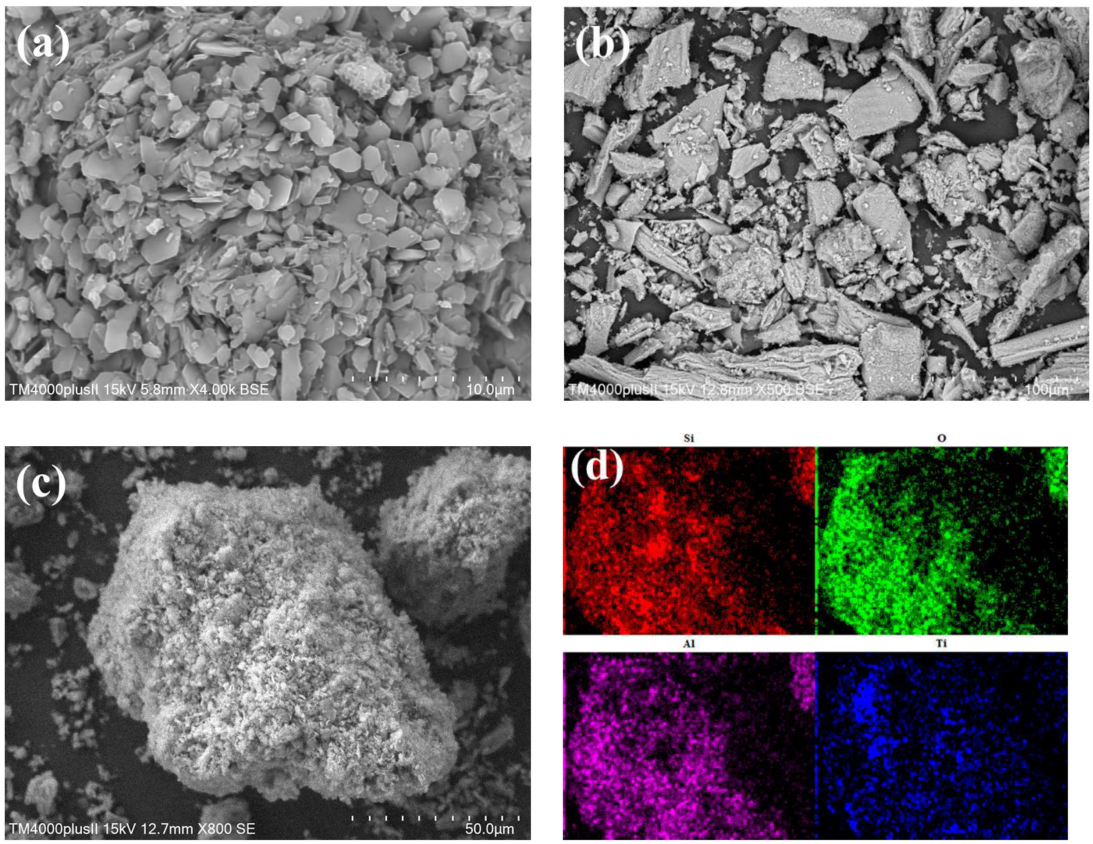

FIGURE 3 | Micro-morphology: **(a)** SEM of zeolite; **(b)** SEM of TiO_2; **(c)** SEM of 500-TZ; **(d)** elements distribution of 500-TZ.

distribution of TiO_2 particles on the surface of zeolite. **Figure 3b** depicts the morphology of pure TiO_2, after thermal treatment the nano-structure of TiO_2 is not observed and it presents a block-shape. This indicates that if nano-TiO_2 particles were not dispersed evenly and anchored firmly, they are prone to agglomerate, thus forming a densified structure and reducing its surface area. The rough surface of zeolite combined with the nano-structure of TiO_2 provides a possibility to synthesize the zeolite supported nano-TiO_2 composite (Ito et al., 2014; Maraschi et al., 2014). In **Figure 3c**, the surface of 500-TZ is coated with a flocculent layer and the edges and corners of zeolite gradually disappear after loading TiO_2, suggesting that porous TiO_2 had been mounted on the surface of zeolite. **Figure 3d** presents the primary elements distribution of TZ-500 (Si, O, Al, and Ti), Ti element is well dispersed on the surface of 500-TZ, further confirming the existence of TiO_2 and the homogeneous distribution of TiO_2. The unique structure of TZ-500 is attributed to TiO_2 modification. More specifically, in the TiO_2 sol, nano-TiO_2 particles existed stably due to the electrostatic repulsion. When heating TiO_2 sol, water was evaporated and surface charge was changed, and thus TiO_2 particles agglomerated. However, when zeolite was immersed in TiO_2 sol, the micro-nano structure of zeolite interacted with TiO_2 under the action of surface charge, nano-TiO_2 particles were fixed on the surface of zeolite, and zeolite provided a large surface to disperse TiO_2 particles. Upon heating, water was evaporated, but TiO_2 particles will not get into agglomeration due to the anchoring of zeolite (Easwaramoorthi and Natarajan, 2009).

BET Analysis

Figure 4A displays isotherm adsorption-desorption curves of as-prepared samples. Hysteresis loops were observed in all samples, confirming the existence of mesoporous structure (Sing et al., 1985), but the shape of isotherms was different, indicating that the pore structure and surface property were altered through thermal treatment under different temperatures. At low relative pressure (<0.5), the N_2 adsorption volume of 200-TZ was approximate to that of 300-TZ and 400-TZ, but higher than that of 500-TZ. This demonstrates that the adsorption ability of 200-TZ, 300-TZ, and 400-TZ was higher that of 500-TZ, which was also verified by the results of SSA in **Figure 4C**. In general, the higher the SSA is, the stronger the adsorption capacity is. It proves that thermal treatment can lead to an agglomeration of TiO_2, thus reducing its SSA, and the higher the temperature is, and more serious the agglomeration is. However, at high relative pressure (>0.5), the N_2 adsorption volume of 200-TZ was noticeably lower than that of 300-TZ, 400-TZ, and 500-TZ. This is probably caused by the pore size difference. As shown in **Figure 4B**, the most probable pore diameter shifted right with temperature, and 200-TZ had

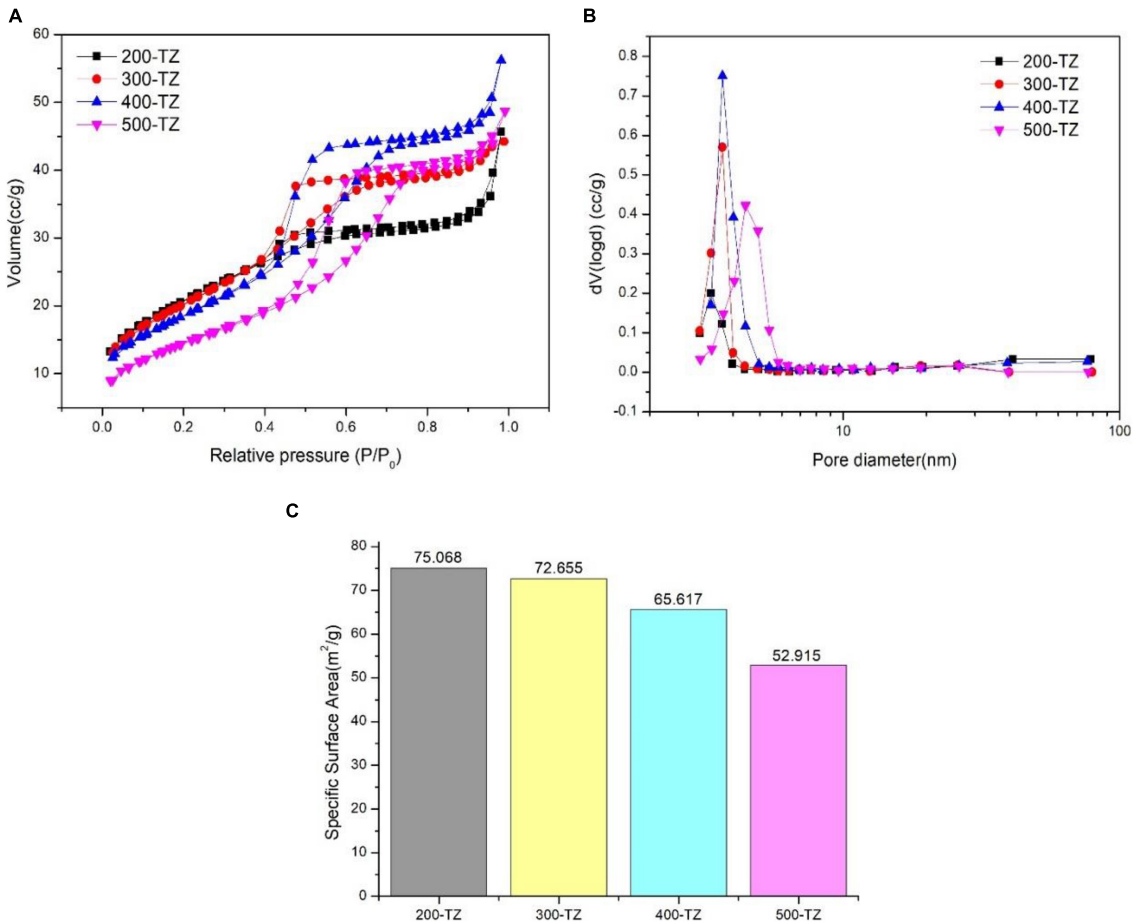

FIGURE 4 | BET analysis results: **(A)** isotherm adsorption-desorption curve; **(B)** pore size distribution curve; **(C)** specific surface area diagram.

the smallest pore diameter (about 3.5 nm). This phenomenon also verified the TiO_2 agglomeration resulted by thermal treatment.

Photocatalytic Degradation of TCAcAm

It is well known that photocatalytic degradation contains three main processes: mass transfer, interphase adsorption, and photocatalytic oxidation. **Figure 5** compares different samples in terms of adsorption rate toward TCAcAm without light. The adsorption rate increased with time and stayed constant after 5 h. And the stable adsorption rate of 200-TZ-25-PCM reached up to about 50%, which was higher than that of zeolite-PCM and TiO_2-PCM. This can be explained by the fact that, although zeolite is porous and has good adsorption capacity, after loading TiO_2 its pore structure was modified, so the adsorption capacity of 200-TZ-25-PCM was enhanced. On the other hand, compared with TiO_2-PCM, 200-TZ-25-PCM can disperse TiO_2 more evenly on the surface of cement paste and provide more adsorption sites, thus leading to a higher adsorption rate.

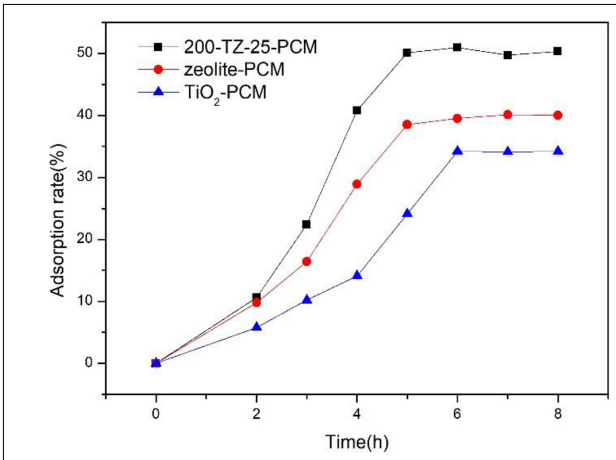

FIGURE 5 | TCAcAm adsorption rate of TiO_2, Zeolite, and 200-TZ-25-PCM.

Figure 6 displays the effect of calcination temperature on the photocatalytic degradation rate toward TCAcAm. The degradation rate was the highest at 200°C (97.6%), and it gradually decreased as the calcination temperature increased. It shows that the prepared photocatalytic PCM has the greatest photocatalytic activity under the calcination condition of 200°C. Because as the temperature increases, the size of the TiO_2@zeolite

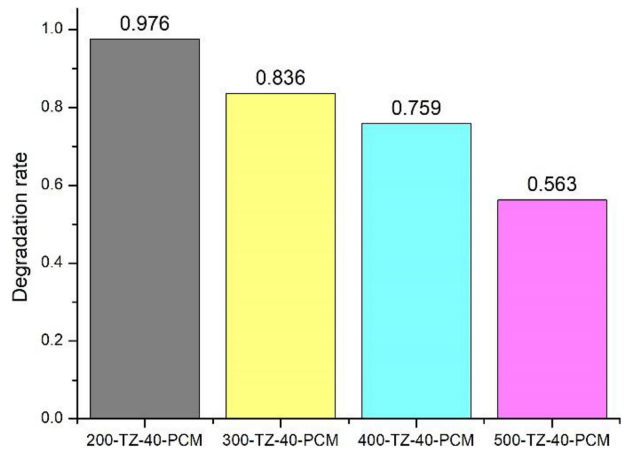

FIGURE 6 | Effect of temperature on degradation rate.

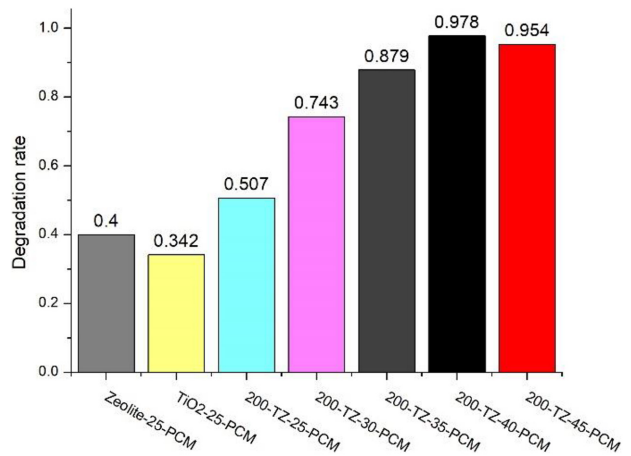

FIGURE 7 | Effect of TiO_2 content on degradation rate.

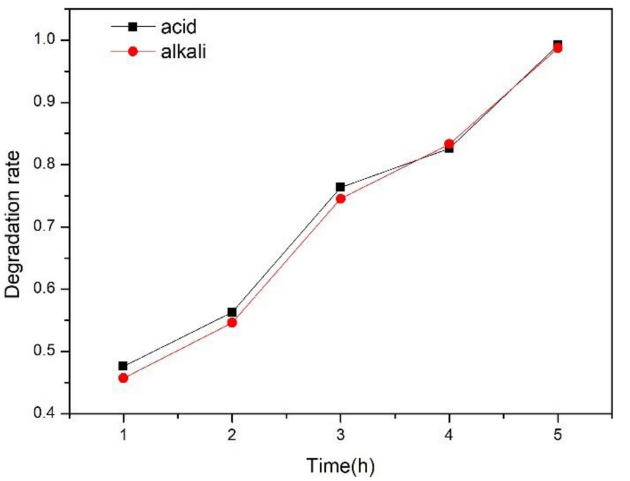

FIGURE 8 | Degradation rate of 200-TZ-40-PCM toward TCAcAm under different pH values.

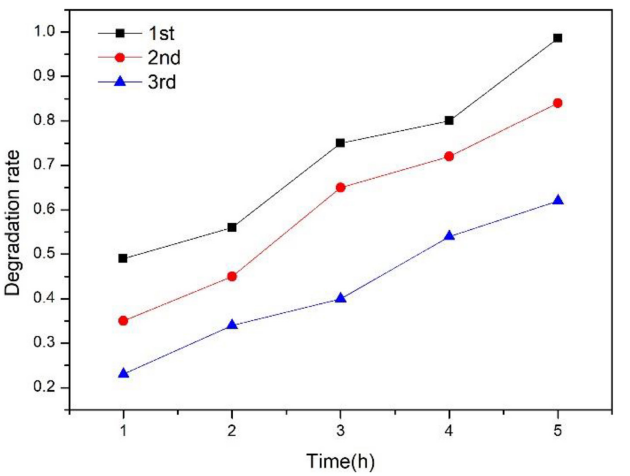

FIGURE 9 | Cycling degradation rate of 200-TZ-40-PCM.

composite particles became larger, resulting in the redshift of the optical energy gap, and the redox potential of electrons/holes became lower, and the activity of the catalyst decreased (Poon and Cheung, 2007).

Figure 7 shows the results of photodegradation of TCAcAm on PCM with different TiO_2 content after 5 h of light. Zeolite-25-PCM stands that the TiO_2 content was 0, and TiO_2-25-PCM stands that the TiO_2 content was 100%. It can be seen that the degradation rates of Zeolite-25-PCM and TiO_2-25-PCM were relatively low, reaching 40 and 34.2%, respectively. The degradation rate of Zeolite-25-PCM was almost equal to its adsorption rate, indicating that Zeolite-25-PCM can only adsorb TCAcAm under light, and TiO_2 particles will get into agglomeration in the cement hydration environment, so the degradation rate of TiO_2-25-PCM was the lowest (34.2%). At low TiO_2 addition, its photocatalytic degradation effect is poor and the adsorption governs the reaction, so the degradation rate of TiO_2-25-PCM was lower than that of Zeolite-25-PCM. Moreover, the degradation rate of 200-TZ-25-PCM was close to its adsorption rate as shown in **Figure 5**. With TiO_2 content increased, the degradation rate rose rapidly, and it reached its highest point (97.8%) as TiO_2@zeolite composite content was 40%. This was owned to two effects. Firstly, the abundant channels and pores, and the large SSAs of zeolite benefited the mass transfer and adsorption. Secondly, the zeolite was an optimal support for TiO_2 due to the unique pore shape, internal pore volume, and channel size (Hashimoto, 2003; Matsuoka and Anpo, 2003; Corma and Garcia, 2004), and TiO_2 was proved to be homogeneously dispersed on the surface of the TiO_2@zeolite composite as the results of N_2 adsorption-desorption and SEM-EDS indicated, thus more active sites were provided. The synergistic effect led to a high photocatalytic efficiency. It should be noticed that the degradation rate of 200-TZ-45-PCM was lower than 200-TZ-40-PCM. This can be explained by the fact that when the content of TiO_2@zeolite composite was high,

it could not be dispersed homogenously on the surface of cement and some active sites will be covered, so its photocatalyic degradation rate was lower even if it had higher TiO_2 content. The intermediate carrier method is effective to improve the photocatalytic performance of the PCM.

It can be seen from **Figure 8** that the degradation rate of 200-TZ-40-PCM toward TCAcAm can reach 98.7 and 99.2% at 5 h under acidic (pH = 5) and alkaline conditions (pH = 11), respectively. It shows that in the process of photocatalytic degradation of TCAcAm, the initial pH has little effect on the degradation rate. The reasons for the above phenomenon may be as follows: the pH value of the solution is an important factor that determines the physical and chemical species in the solution and the state of the molecules in the solution. In the case of acidic initial conditions (pH = 5) and alkaline initial conditions (pH = 11), since the pKa value of TCAcAm is 8.75, when the pH value of the solution was lower than 9, TCAcAm existed in the form of $C_2H_2Cl_3NO$ molecules, and as the pH value was lower than 8.75, it existed in the form of $C_2HCl_3NO^-$. Therefore, regardless of acidic or alkaline conditions, TiO_2 had no additional adsorption effect on TCAcAm due to the protonation of the charge on the TiO_2 surface, so acidity and alkalinity have no great effect on the photocatalytic degradation of TCAcAm.

The results of the recycle degradation experiment of 200-TZ-40-PCM are shown in **Figure 9**. The first degradation rate reached up to 98.6% for TCAcAm within 5 h. However, from the second cycle onward, the degradation rate decreased slightly. When the tests were recycled three times, the third degradation rate was 56.6%. The decrease in degradation rate is probably due to the occupation of TiO_2 active sites by TCAcAm or the reaction products.

CONCLUSION

(1) Through the sol-gel method, TiO_2@zeolite composite catalyst was successfully prepared. SEM images and BET results showed that zeolite was porous and had large SSA. XRD and EDS results confirmed that nano-TiO_2 particles were homogeneously dispersed on the surface of zeolite.

(2) TiO_2@zeolite composite coated PCM had excellent adsorption ability. The synergistic effect of the surface adsorption of zeolite and the photocatalytic degradation of TiO_2 can significantly improve the photocatalytic degradation performance of the TiO_2@zeolite composite coated PCM. 200-TZ-40-PCM (TiO_2@zeolite composite content was 40% and thermal treatment temperature was 200°C) had the highest degradation rate (97.8%) within 5 h, which was about 2.86 times than pure TiO_2 coated PCM.

(3) The TCAcAm degradation rate was regardless of pH value, and decreased with thermal treatment temperature. After several repeated experiments, the degradation rate had a declining trend.

DATA AVAILABILITY STATEMENT

The original contributions presented in the study are included in the article/supplementary material, further inquiries can be directed to the corresponding author/s.

AUTHOR CONTRIBUTIONS

GL: literature search, figures, and writing. WC: data collection. JZ: data analysis. WY: study design. AS: funding and data interpretation. All authors contributed to the article and approved the submitted version.

FUNDING

This work was supported by the National Key R&D Program of China (grant no. 2019YFC1906203) and the National Natural Science Foundation of China (grant no. 51108341).

REFERENCES

Ahmed, S., Rasul, M., Martens, W. N., Brown, R., and Hashib, M. (2010). Heterogeneous photocatalytic degradation of phenols in wastewater: a review on current status and developments. *Desalination* 261, 3–18. doi: 10.1016/j.desal.2010.04.062

Aïssa, A. H., Puzenat, E., Plassais, A., Herrmann, J.-M., Haehnel, C., and Guillard, C. (2011). Characterization and photocatalytic performance in air of cementitious materials containing TiO_2. Case study of formaldehyde removal. *Appl. Catal. B Environ.* 107, 1–8. doi: 10.1016/j.apcatb.2011.06.012

Chang, H., Chen, C., and Wang, G. (2013). Characteristics of C-, N-DBPs formation from nitrogen-enriched dissolved organic matter in raw water and treated wastewater effluent. *Water Res.* 47, 2729–2741. doi: 10.1016/j.watres.2013.02.033

Chen, J., Kou, S.-C., and Poon, C.-S. (2011). Photocatalytic cement-based materials: comparison of nitrogen oxides and toluene removal potentials and evaluation of self-cleaning performance. *Build. Environ.* 46, 1827–1833. doi: 10.1016/j.buildenv.2011.03.004

Chen, J., and Poon, C.-S. (2009). Photocatalytic cementitious materials: influence of the microstructure of cement paste on photocatalytic pollution degradation. *Environ. Sci. Technol.* 43, 8948–8952. doi: 10.1021/es902359s

Chu, W., Gao, N., Krasner, S. W., Templeton, M. R., and Yin, D. (2012). Formation of halogenated C-, N-DBPs from chlor (am) ination and UV irradiation of tyrosine in drinking water. *Environ. Pollut.* 161, 8–14. doi: 10.1016/j.envpol.2011.09.037

Corma, A., and Garcia, H. (2004). Zeolite-based photocatalysts. *Chem. Commun.* 35, 1443–1459. doi: 10.1039/b400147h

Easwaramoorthi, S., and Natarajan, P. (2009). Characterisation and spectral properties of surface adsorbed phenosafranine dye in zeolite-Y and ZSM-5: photosensitisation of embedded nanoparticles of titanium dioxide. *Microporous Mesoporous Mater.* 117, 541–550. doi: 10.1016/j.micromeso.2008.07.042

Fuchs, V., Méndez, L., Blanco, M., and Pizzio, L. (2009). Mesoporous titania directly modified with tungstophosphoric acid: synthesis, characterization and catalytic evaluation. *Appl. Catal. A Gen.* 358, 73–78. doi: 10.1016/j.apcata.2009.01.040

Fujishima, A., and Honda, K. (1972). Electrochemical photolysis of water at a semiconductor electrode. *Nature* 238, 37–38. doi: 10.1038/238037a0

Hashimoto, S. (2003). Zeolite photochemistry: impact of zeolites on photochemistry and feedback from photochemistry to zeolite science. *J. Photochem. Photobiol. C Photochem. Rev.* 4, 19–49. doi: 10.1016/s1389-5567(03)00003-0

Hom, L. W. (1972). Kinetics of chlorine disinfection in an ecosystem. *J. Sanit. Eng. Div.* 98, 183–194. doi: 10.1061/jsedai.0001370

Ito, M., Fukahori, S., and Fujiwara, T. (2014). Adsorptive removal and photocatalytic decomposition of sulfamethazine in secondary effluent using TiO_2-zeolite composites. *Environ. Sci. Pollut. Res.* 21, 834–842. doi: 10.1007/s11356-013-1707-9

Jansson, I., Suárez, S., Garcia-Garcia, F. J., and Sánchez, B. (2015). Zeolite-TiO_2 hybrid composites for pollutant degradation in gas phase. *Appl. Catal. B Environ.* 178, 100–107. doi: 10.1016/j.apcatb.2014.10.022

Jimenez-Relinque, E., Rodriguez-Garcia, J., Castillo, A., and Castellote, M. (2015). Characteristics and efficiency of photocatalytic cementitious materials: type of binder, roughness and microstructure. *Cem. Concr. Res.* 71, 124–131. doi: 10.1016/j.cemconres.2015.02.003

Karuppuchamy, S., Iwasaki, M., and Minoura, H. (2007). Physico-chemical, photoelectrochemical and photocatalytic properties of electrodeposited nanocrystalline titanium dioxide thin films. *Vacuum* 81, 708–712. doi: 10.1016/j.vacuum.2006.09.013

Lee, B. Y., Jayapalan, A. R., and Kurtis, K. E. (2013). Effects of nano-TiO_2 on properties of cement-based materials. *Mag. Concr. Res.* 65, 1293–1302.

Liu, X., Steele, J. C., and Meng, X.-Z. (2017). Usage, residue, and human health risk of antibiotics in Chinese aquaculture: a review. *Environ. Pollut.* 223, 161–169. doi: 10.1016/j.envpol.2017.01.003

Maraschi, F., Sturini, M., Speltini, A., Pretali, L., Profumo, A., Pastorello, A., et al. (2014). TiO_2-modified zeolites for fluoroquinolones removal from wastewaters and reuse after solar light regeneration. *J. Environ. Chem. Eng.* 2, 2170–2176. doi: 10.1016/j.jece.2014.08.009

Matsuoka, M., and Anpo, M. (2003). Local structures, excited states, and photocatalytic reactivities of highly dispersed catalysts constructed within zeolites. *J. Photochem. Photobiol. C Photochem. Rev.* 3, 225–252. doi: 10.1016/s1389-5567(02)00040-0

Nazari, A., and Riahi, S. (2011). RETRACTED: the effects of TiO_2 nanoparticles on properties of binary blended concrete. *J. Compos. Mater.* 45, 1181–1188. doi: 10.1177/0021998310378910

Negishi, N., Miyazaki, Y., Kato, S., and Yang, Y. (2019a). Effect of HCO_3-concentration in groundwater on TiO_2 photocatalytic water purification. *Appl. Catal. B Environ.* 242, 449–459. doi: 10.1016/j.apcatb.2018.10.022

Negishi, N., Sugasawa, M., Miyazaki, Y., Hirami, Y., and Koura, S. (2019b). Effect of dissolved silica on photocatalytic water purification with a TiO_2 ceramic catalyst. *Water Res.* 150, 40–46. doi: 10.1016/j.watres.2018.11.047

Pawar, M., Topcu Sendoğdular, S., and Gouma, P. (2018). A brief overview of TiO_2 photocatalyst for organic dye remediation: case study of reaction mechanisms involved in Ce-TiO_2 photocatalysts system. *J. Nanomater.* 2018:5953609.

Poon, C. S., and Cheung, E. (2007). NO removal efficiency of photocatalytic paving blocks prepared with recycled materials. *Constr. Build. Mater.* 21, 1746–1753. doi: 10.1016/j.conbuildmat.2006.05.018

Seo, D., and Yun, T. S. (2017). NOx removal rate of photocatalytic cementitious materials with TiO_2 in wet condition. *Build. Environ.* 112, 233–240. doi: 10.1016/j.buildenv.2016.11.037

Sing, K. S., Everett, D., Haul, R., Moscou, L., Pierotti, R., Rouquerol, J., et al. (1985). Reporting physisorption data for gas/solid systems with special reference to the determination of surface area and porosity (Recommendations 1984). *Pure Appl. Chem.* 57, 603–619. doi: 10.1351/pac198557040603

Srogi, K. (2007). Monitoring of environmental exposure to polycyclic aromatic hydrocarbons: a review. *Environ. Chem. Lett.* 5, 169–195. doi: 10.1007/s10311-007-0095-0

Vinu, R., and Madras, G. (2012). Environmental remediation by photocatalysis. *J. Indian Inst. Sci.* 90, 189–230.

Wang, J., Lu, C. H., and Xiong, J. R. (2014). Self-cleaning and depollution of fiber reinforced cement materials modified by neutral TiO2/SiO2 hydrosol photoactive coatings[J]. *Appl. Surf. Sci.* 298, 19–25.

Wen, M., Zhang, S., Dai, W., Li, G., and Zhang, D. (2015). In situ synthesis of Ti^{3+} self-doped mesoporous TiO2 as a durable photocatalyst for environmental remediation. *Chin. J. Catal.* 36, 2095–2102. doi: 10.1016/s1872-2067(15)60992-5

Whelton, A. J., McMillan, L., Connell, M., Kelley, K. M., Gill, J. P., White, K. D., et al. (2015). Residential tap water contamination following the freedom industries chemical spill: perceptions, water quality, and health impacts. *Environ. Sci. Technol.* 49, 813–823. doi: 10.1021/es5040969

Winward, G. P., Avery, L. M., Stephenson, T., and Jefferson, B. (2008). Chlorine disinfection of grey water for reuse: effect of organics and particles. *Water Res.* 42, 483–491. doi: 10.1016/j.watres.2007.07.042

Yamaguchi, S., Fukura, T., Imai, Y., Yamaura, H., and Yahiro, H. (2010). Photocatalytic activities for partial oxidation of α-methylstyrene over zeolite-supported titanium dioxide and the influence of water addition to reaction solvent. *Electrochim. Acta* 55, 7745–7750. doi: 10.1016/j.electacta.2009.11.091

Yoneyama, H., and Torimoto, T. (2000). Titanium dioxide/adsorbent hybrid photocatalysts for photodestruction of organic substances of dilute concentrations. *Catal. Today* 58, 133–140. doi: 10.1016/s0920-5861(00)00248-0

Zangeneh, H., Zinatizadeh, A., Habibi, M., Akia, M., and Isa, M. H. (2015). Photocatalytic oxidation of organic dyes and pollutants in wastewater using different modified titanium dioxides: a comparative review. *J. Ind. Eng. Chem.* 26, 1–36. doi: 10.1016/j.jiec.2014.10.043

Zhang, L., Kanki, T., Sano, N., and Toyoda, A. (2003). Development of TiO_2 photocatalyst reaction for water purification. *Sep. Purif. Technol.* 31, 105–110. doi: 10.1016/s1383-5866(02)00157-0

Conflict of Interest: JZ was employed by the company Shanghai Construction Group Co., Ltd., Shanghai, China.

The remaining authors declare that the research was conducted in the absence of any commercial or financial relationships that could be construed as a potential conflict of interest.